



Signal strength and climate calibration of a European tree-ring isotope network

K. Treydte,¹ D. Frank,¹ J. Esper,¹ L. Andreu,² Z. Bednarz,³ F. Berninger,⁴ T. Boettger,⁵ C. M. D'Alessandro,⁶ N. Etien,⁷ M. Filot,⁸ M. Grabner,⁹ M. T. Guillemain,⁷ E. Gutierrez,² M. Haupt,⁵ G. Helle,¹⁹ E. Hiltavuori,¹⁰ H. Jungner,¹⁰ M. Kalela-Brundin,¹¹ M. Krapiec,¹² M. Leuenberger,⁸ N. J. Loader,¹³ V. Masson-Delmotte,⁷ A. Pazdur,¹⁴ S. Pawelczyk,¹⁴ M. Pierre,⁷ O. Planells,² R. Pukiene,¹⁵ C. E. Reynolds-Henne,¹⁶ K. T. Rinne,¹⁷ A. Saracino,¹⁸ M. Saurer,¹⁶ E. Sonninen,¹⁰ M. Stievenard,⁷ V. R. Switsur,¹⁷ M. Szczepanek,¹⁴ E. Szychowska-Krapiec,¹² L. Todaro,⁶ J. S. Waterhouse,¹⁷ M. Weigl,⁹ and G. H. Schleser¹⁹

Received 20 June 2007; revised 29 August 2007; accepted 5 October 2007; published 19 December 2007.

[1] We present the first European network of tree ring $\delta^{13}\text{C}$ and $\delta^{18}\text{O}$, containing 23 sites from Finland to Morocco. Common climate signals are found over broad climatic-ecological ranges. In temperate regions we find positive correlations with summer maximum temperatures and negative correlations with summer precipitation and Palmer Drought Severity Indices (PDSI) with no obvious species-specific differences. Regional $\delta^{13}\text{C}$ and $\delta^{18}\text{O}$ chronologies share high common variance in year-to-year variations. Long-term variations, however, exhibit differences that may reflect spatial variability in environmental forcings, age trends and/or plant physiological responses to increasing atmospheric CO_2 concentration. Rotated principal component analysis (RPCA) and climate field correlations enable the identification of four sub-regions in the $\delta^{18}\text{O}$ network - northern and eastern Central Europe, Scandinavia and the western Mediterranean. Regional patterns in the $\delta^{13}\text{C}$ network are less clear and are timescale dependent. Our results indicate that future reconstruction efforts should concentrate on $\delta^{18}\text{O}$ data in the identified European regions. **Citation:** Treydte, K., et al. (2007), Signal strength and climate calibration of a European tree-ring isotope network, *Geophys. Res. Lett.*, 34, L24302, doi:10.1029/2007GL031106.

1. Introduction

[2] 21st century global warming and its potential impact on the hydrological cycle [Allen and Ingram, 2002;

Trenberth and Shea, 2005; Treydte et al., 2006] strengthen the need to quantify climate changes particularly in regions with large human populations. Europe represents a region where significant progress has been made in assessing past climate variations due to the availability of long instrumental records, documentary archives, and natural proxies. Temperature and precipitation fields have been reconstructed over the whole European region based primarily on long instrumental records and documentary data [Luterbacher et al., 2004; Pauling et al., 2006; Xoplaki et al., 2005]. Many long-term high-resolution proxy reconstructions are, however, restricted to temperature variations at high latitudes or altitudes [Esper et al., 2002; Büntgen et al., 2006; Frank and Esper, 2005] or to local/regional precipitation or drought variability [e.g., Casty et al., 2005; Masson-Delmotte et al., 2005; Wilson et al., 2005]. This is because the climatic signal in the most prominent proxies - tree ring width and maximum latewood density - is strongest at ecological boundary conditions. Hence, additional proxy records are required, which enable the expansion of climate reconstructions into temperate regions. Local analyses of tree ring stable isotopes have demonstrated potential in providing environmental information from such sites [e.g., Masson-Delmotte et al., 2005; Rafalli-Delerce et al., 2004; Saurer et al., 1997] and therefore could help to overcome some limitations in dendroclimatology [Esper et al., 2005].

[3] Here we present 20th century carbon and oxygen isotope data ($\delta^{13}\text{C}$ and $\delta^{18}\text{O}$) from a network of 23 sites

¹Swiss Federal Research Institute WSL, Birmensdorf, Switzerland.

²Departamento d'Ecologia, Facultat de Biologia, Universitat de Barcelona, Barcelona, Spain.

³Department of Forest Botany, Agricultural University, Krakow, Poland.

⁴Department of Biological Sciences, University of Quebec at Montreal, Montreal, Quebec, Canada.

⁵UFZ-Helmholtz Centre for Environmental Research, Halle/Saale, Germany.

⁶Department of Crop Systems, Forestry, and Environmental Sciences, Università della Basilicata, Potenza, Italy.

⁷Laboratoire des Sciences du Climat et de l'Environnement, L'Orme des Merisiers CEA Saclay IPSL/CEA/CNRS-UVSQ, Gif sur Yvette, France.

⁸Climate and Environmental Physics, Physics Institute, University of Bern, Bern, Switzerland.

⁹Institute of Wood Research, University of Natural Resources and Applied Life Sciences, BOKU, Vienna, Austria.

¹⁰Dating Laboratory, University of Helsinki, Helsinki, Finland.

¹¹Museum of Forestry, Lycksele, Sweden.

¹²Faculty of Geology, Geophysics and Environmental Protection, AGH University of Science and Technology, Krakow, Poland.

¹³Department of Geography, Swansea University, Swansea, UK.

¹⁴Institute of Physics, Silesian University of Technology, Gliwice, Poland.

¹⁵Kaunas Botanical Gardens Lab, Vytautas Magnus University, Kaunas, Lithuania.

¹⁶Paul Scherrer Institut, Villigen, Switzerland.

¹⁷Environmental Sciences Research Centre, Anglia Ruskin University, Cambridge, UK.

¹⁸Department of Arboriculture, Botany and Plant Pathology, University of Naples "Federico II", Portici, Italy.

¹⁹Forschungszentrum Jülich GmbH, Jülich, Germany.

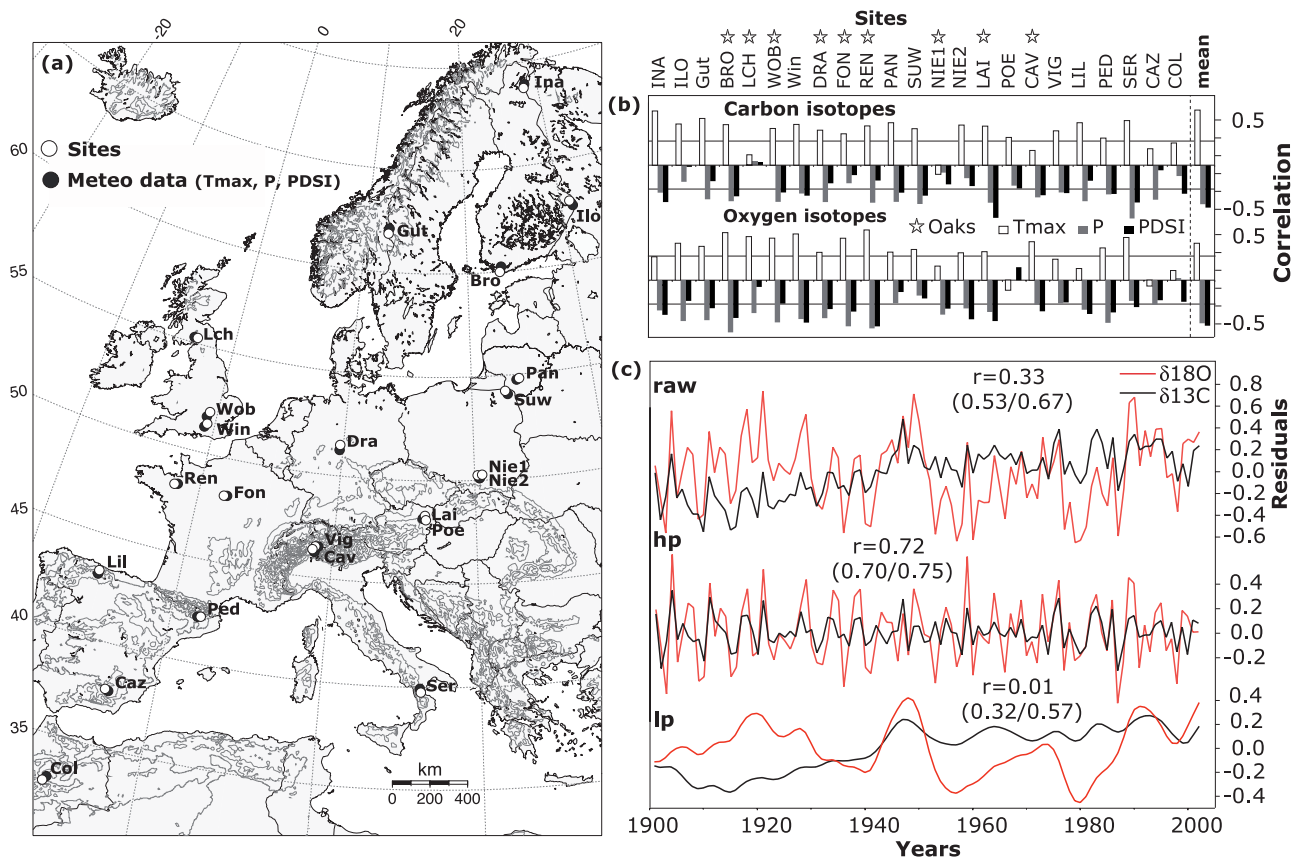


Figure 1. (a) Tree sites and corresponding meteorological grid cells for the 20th century with codes indicating site names. (b) Site dependent June–August climate correlations of ‘raw’ carbon and oxygen isotope chronologies, with sites being latitudinally arranged (for detailed site information, see Table S1); stars indicate oak sites; ‘mean’ are correlations between mean isotope records averaged over all sites and mean meteorological data averaged over corresponding grid cells; and lines are $p < 0.01$ significance levels. (c) ‘European’ carbon and oxygen isotope chronologies (each calculated by averaging site chronologies); ‘raw’ = residuals from 1901–1998 means, hp = high pass filtered data; lp = low pass filtered data; r = Pearson’s correlation coefficient; and numbers in brackets are r -values for the early AD 1901–1951 and the recent AD 1952–2002 period, respectively.

ranging from Fennoscandia to the Mediterranean region. We discuss results from (i) signal strength analyses within the networks, (ii) climate calibration of isotopic parameters to summer conditions, and (iii) spatial network analyses. We detail common variance within European sub-regions and emphasise the reconstruction potential of annually resolved $\delta^{18}O$ from tree rings.

2. Material and Methods

[4] Twenty-three sites ranging from northern Finland to Morocco with $\delta^{13}C$ and $\delta^{18}O$ chronologies from three genera (*Quercus*, *Pinus*, *Cedrus*) were included in the analysis (Figure 1a and Table S1). The sampling design considered not only ecologically extreme sites, with a single climatic factor dominating tree growth, but also temperate sites where mixed climate signals are recorded in tree ring width and maximum latewood density. All chronologies cover the 1901–1998 period, with 20 sites extending to 2002. Ring widths were measured and tree rings cross-dated following standard procedures [Fritts, 1976]. At least four dominant trees per site (two cores per tree) were selected for isotope analysis, a number proven to be satisfactory to

develop a (population-) representative isotope site record [Leavitt and Long, 1984; McCarroll and Loader, 2004; Gagen et al., 2004; Treydte et al., 2001, 2006].

[5] Pine and cedar tree rings were separated year-by-year, whilst for oak latewood was analysed (except CAV, where no separation in early and latewood was possible owing to the extreme narrowness of the latewood). At most sites, all tree rings from the same year were pooled prior to cellulose extraction to provide enough matter for isotopic analysis [Leavitt and Long, 1984; Treydte et al., 2001]. Alpha-cellulose was extracted following standardized procedures [Boettger et al., 2007] and combusted to CO_2 or pyrolysed to CO, prior to mass spectrometer analysis. $\delta^{18}O$ values are expressed as deviations from the VSMOW and $\delta^{13}C$ values as deviations from the VPDB standards. $\delta^{13}C$ records were corrected for the atmospheric $\delta^{13}C$ decrease due to fossil fuel burning since the beginning of industrialisation [McCarroll and Loader, 2004]. Initially all isotope series were screened for missing values and gaps filled using information from adjacent chronologies [Pederson et al., 2004]. Signal strength analyses were conducted on high pass (hp) and low pass (lp) filtered data using cubic smoothing splines

with 50% frequency-response cut-off at 10 years [Cook and Peters, 1981] for frequency decomposition.

[6] Climate calibration was performed using an updated version of the $0.5^\circ \times 0.5^\circ$ monthly gridded meteorological data set CRU TS 2.1 [Mitchell and Jones, 2005]. Analyses considered mean, minimum and maximum temperatures, precipitation, wet day frequencies and vapour pressure. Here we focus on the highest correlations observed for maximum temperatures (T_{\max}) and precipitation (P). Additionally, a newly developed European $0.5^\circ \times 0.5^\circ$ grid of monthly resolved Palmer Drought Severity Index data (PDSI) is used for calibration [van der Schrier et al., 2006; Wells et al., 2004] as well as a $2.5^\circ \times 2.5^\circ$ grid of PDSI data [Dai et al., 2004], accessed via the KMNI climate explorer (<http://climexp.knmi.nl>).

3. Results

[7] 20th century mean values of the individual $\delta^{13}\text{C}$ site chronologies span 5.1 ‰ with lowest values recorded at the Polish site ‘Nie2’ and highest values in Morocco (‘Col’). Lowest $\delta^{18}\text{O}$ means are found at the Finnish site ‘Bro’ and highest values at the Spanish site ‘Caz’ and again at the Moroccan site ‘Col’ differing by 7.9 ‰ (Table S1). Mean inter-site correlations for the residual as well as for the hp and lp records indicate little common variance in the overall isotope networks, although correlations are slightly higher for $\delta^{18}\text{O}$ (records and values shown in Figure S1¹). This result is not surprising, considering the large region covered, yet the question remains whether different climate sensitivity at individual sites or regional differences in climate variability are responsible for the low inter-site correlations.

[8] On a site basis, the strongest responses of both isotope parameters are found with climate variables for the year of tree ring formation, displaying highest correlations with the summer months. Calculations based on different seasonal windows indicate that the number of significantly correlating sites varies depending on the climatic variable and isotopic parameter (Figure S2). Nevertheless, correlation signs of combined June–August (JJA) maximum temperature (positive), precipitation (negative) and PDSI (negative), respectively, are common at the majority of sites, despite the broad climatic and ecological range (Figure 1b). Interestingly, the moisture signal (particularly $\delta^{13}\text{C}$) of the dry sites (Switzerland, Mediterranean) is generally weaker than was expected from some earlier analyses [Warren et al., 2001]. Signals are not only robust between sites but also between isotope parameters. Temperature sensitivity in the $\delta^{18}\text{O}$ network is particularly strong at northern latitudes and at sites influenced by North Atlantic air masses. It has to be noted, that on the ‘site’ as well as on the ‘European’ scale, high correlations to several climate variables are partly based on systematic associations between the target variables themselves, particularly during summer. All European JJA records are significantly ($p < 0.001$) correlated with each other: $T_{\max} - P$ at $r = -0.41$, $T_{\max} - \text{PDSI}$ at $r = -0.39$ and $P - \text{PDSI}$ at $r = 0.50$.

[9] Previous year conditions do not have a strong effect on either carbon or oxygen isotope values (Figure S2). This finding was somewhat expected for the latewood cellulose from oak, but interestingly also holds for pine (whole ring cellulose) and, thus, does not indicate substantial carry-over effects in conifers due to remobilized reserves from previous summer [Kagawa et al., 2006; Helle and Schleser, 2004].

[10] A grand mean over all site records and comparison with corresponding instrumental data provides an indication of the common climatic variance emphasised by combining numerous sites. (Figure 1b). Particularly the temperature signal in the $\delta^{13}\text{C}$ network ($r = 0.61$) and the PDSI signal in the $\delta^{18}\text{O}$ network ($r = -0.51$) are higher than most individual site correlations, with the latter even increasing when based on hp data ($r = -0.66$; Figure S3). Comparisons of the ‘European’ $\delta^{13}\text{C}$ and $\delta^{18}\text{O}$ chronologies indicate strong and temporally robust coherence in the higher frequency domain. Discrepancies, however, can be found in the longer-term trends with increasing $\delta^{13}\text{C}$, particularly in the first half of the 20th century, and more decadal variation in $\delta^{18}\text{O}$ (Figure 1c).

[11] To analyse spatial coherence within the isotope networks, principal component analysis (PCA) was applied. The first five PCs containing 56% of the variance in the $\delta^{13}\text{C}$ and 57% of the variance in the $\delta^{18}\text{O}$ network were retained and subjected to Varimax Rotation [Richman, 1986]. The rotated principal components (RPC) of the $\delta^{18}\text{O}$ network seem to be largely independent of species and allow the identification of regional subsets using the highest loadings on the first four axes: The first rotated factor (RPC1) explains 18% of the variance with highest loadings of the northern Central European sites in the UK and France (mean loading = 0.71) and moderately high loadings of the oaks from the Swiss Alps (0.47, ‘Cav’) and Austria (0.58, ‘Lai’). Loadings on RPC2 (12% variance explained) are highest at the four eastern Central European sites and the Austrian pine site ‘Poe’ (mean loading = 0.62) and moderately high at the German (0.49, ‘Dra’) and Italian sites (0.50, ‘Ser’). RPC3 (11%) shows highest loadings at all Scandinavian sites (mean loading = 0.63) with the northernmost site ‘Ina’ contributing less (0.48). Finally, loadings on RPC4 (8%) are highest in the western Mediterranean region (mean loading = 0.61) and at the Swiss pine site ‘Vig’ (0.60) and moderately high at the southernmost Spanish site ‘Caz’ (0.53). As only ‘Col’ from Morocco loads most strongly on RPC5 (7%), this component is not further detailed here. Interestingly the identified sub-groups are identical for the RPCs derived from high pass filtered $\delta^{18}\text{O}$ records, and hence are robust over different frequencies. In contrast, RPC patterns of the $\delta^{13}\text{C}$ chronologies are much more diffuse and timescale dependent (not shown), a result that we attribute to more site-specific variance and/or complex long-term behaviour of this parameter.

[12] Comparison of the most relevant principal components with European climate field data (Figure 2) revealed strongest influences of all climate variables during JJA on RPC1 and 3 and slightly shifted maximum temperature response seasons for RPC2 (JAS) and 4 (MJJ). Generally, the spatial distribution of the highest loading sites nicely corresponds with the climate correlation patterns (see the colours in Figure 2). This holds particularly for RPC1,

¹Auxiliary materials are available in the HTML. doi:10.1029/2007GL031106.

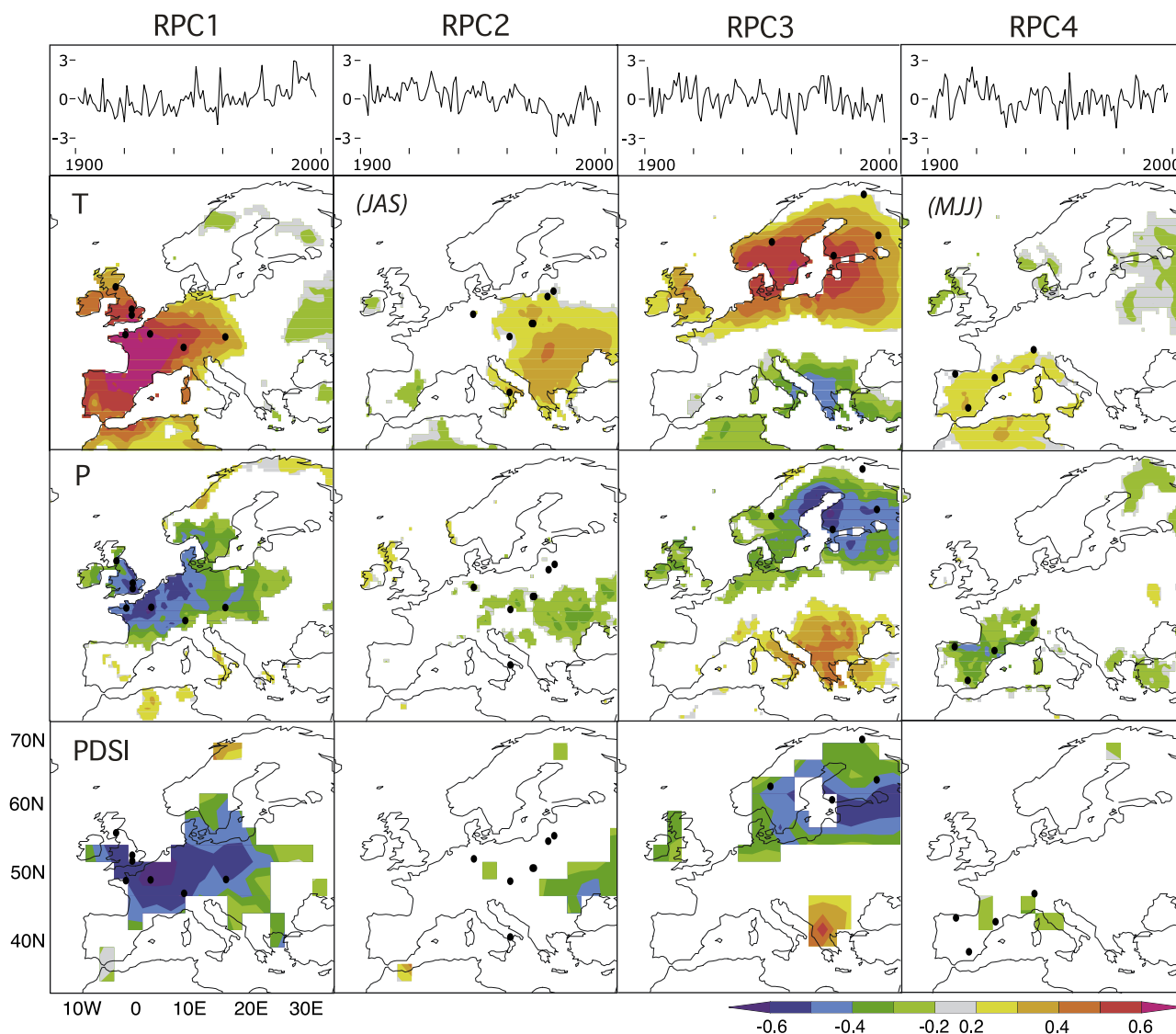


Figure 2. Maps of loadings of site chronologies on varimax-rotated principal components, for the first four of five retained $\delta^{18}\text{O}$ chronology factors (RPC1-4) and corresponding spatial correlation fields for temperature (T), precipitation (P), and PDSI. Dots are sites participating with highest loadings at the corresponding RPCs (time series shown top). Correlations were calculated with seasonal means of June–August (JJA), if not noted differently (*JAS* = July to September, *MJJ* = May to June). All calculations are based on the 1901–1998 common period.

representing Northern and Central European conditions and RPC3, correlating closely with a broad area in North-eastern Europe. RPC4 matches JJA temperature and precipitation over the western Mediterranean Region, whereas RPC2 - with contributing tree sites weighted towards a central European transition zone - shows only weak correlations with the instrumental variables tested.

[13] Altogether, temperatures yield the highest correlations and spatially the most homogenous patterns, which can be explained by the spatial homogeneity of this variable itself. Precipitation signals are patchier, but particularly for RPC1 correspond more closely to the region covered by the relevant tree sites. The PDSI patterns, especially for RPC1 and RPC3, cover the broadest areas, and appear relatively homogenous. This homogeneity is, however, affected by the coarser resolution of the PDSI grid and increased dependency of individual grid cells due to the inclusion of

temperature and soil type information [Dai *et al.*, 2004]. Strongest correlations to all climate variables over northern Central Europe (RPC1) are probably due to a concentration of sites in this region which additionally show rather strong climate signals on a site basis (Figure 1b).

4. Discussion

[14] Despite different sources and fractionation processes driving C and O isotope values in tree rings, surprisingly strong similarities in the response of $\delta^{13}\text{C}$ and $\delta^{18}\text{O}$ networks to summer climate conditions are found. Tree ring $\delta^{13}\text{C}$ values depend on diffusion and biochemical processes during photosynthetic CO_2 assimilation, with fractionation effects occurring through the diffusion of CO_2 into the stomata and through enzymatic processes during carbon fixation by Rubisco [Farquhar *et al.*, 1982]. $\delta^{18}\text{O}$ values

largely depend on $\delta^{18}\text{O}$ of soil water, which itself is related to the isotope value of rain water, residence time in the soil, evaporation effects and leaf water enrichment due to transpiration at the stomata [Yakir and Sternberg, 2000]. Therefore, both isotope parameters are linked through effects at the leaf level, mediated through variation in stomatal conductance caused by the combined effect of varying temperature and precipitation conditions. Low stomatal conductance during dry/warm weather conditions causes high $\delta^{13}\text{C}$ values through reduced discrimination against ^{13}C . At the same time low relative humidity and high transpiration rates, due to a larger vapour pressure deficit, increase the leaf water enrichment and thus result in higher $\delta^{18}\text{O}$ values [Masson-Delmotte et al., 2005; Rafalli-Delerce et al., 2004; Roden et al., 2000; Saurer et al., 1997]. Hence, particularly under temperate conditions, both parameters are mainly related to summer moisture conditions. Altogether, these mechanisms drive the strong positive correlations to maximum temperature, which represents relevant daytime conditions slightly better than mean temperature (0.02 higher correlations to both isotope parameters than T_{mean} , averaged over all sites) and negative correlations to precipitation in our data. However, since particularly in Central Europe both variables are strongly inter-correlated during summer, the integrating PDSI might be the most appropriate parameter for reconstructing past climatic-ecological conditions, when including both isotope parameters in one model. A clearer focus on drought reconstructions using stable isotopes would also fill a current research gap in high-resolution palaeoclimatology, as such records are rare for temperate regions [Wilson et al., 2005]. Nevertheless, there is still the need to better disentangle mixed temperature and precipitation influences on isotopic discrimination.

[15] Using PCA we highlight the potential of the $\delta^{18}\text{O}$ network for climate reconstruction in four distinct European sub-regions. The retrieved west-east and north-south gradients and the close association of tree ring $\delta^{18}\text{O}$ with precipitation and temperature regimes support the theory of isotopic fractionation as functions of air mass sourcing (temperature of condensation) and air mass trajectory [Rozanski et al., 1993]. The less distinct regional patterns in the $\delta^{13}\text{C}$ network, which are also wavelength dependent, as well as the discrepancies between $\delta^{13}\text{C}$ and $\delta^{18}\text{O}$ records in the low frequency domain, are, however, not yet understood. It is possible that they are related to more local climatic and/or ecological conditions and trends, but could also result from long-term biases within the isotope records through individual age-related trends, site-dependent changes in the physiological response to increasing CO_2 , or currently unexplainable noise [Treydte et al., 2001, 2006]. Once the problem of differing long-term trends is solved, the approach of combining both isotopes may yield relationships that are less influenced by physiological disturbances [Loader et al., 2007], thereby further enhancing the climate signal (Text S1 and Figure S4).

[16] Our results demonstrate the utility of isotopes in tree rings as an additional proxy for climate reconstruction over Europe. While slightly higher correlations may be obtained for temperature, the physiological mechanisms responsible for isotopic discrimination, reflecting a mixture of temperature and moisture influences, point to the PDSI as a key parameter for climatic reconstruction.

[17] **Acknowledgments.** This project was supported by the European Union (EVK2-CT-2002-00147 'ISONET' and GOCE 017008-2 'MILLENNIUM'). Figure 2 was generated using the KNMI climate explorer (<http://climexp.knmi.nl>). We are grateful to Tim Osborn, Bill Patterson, and two anonymous reviewers for their constructive comments and suggested improvements to the manuscript. NJL acknowledges support from the UK NERC NE/B501504/1.

References

- Allen, M. R., and W. J. Ingram (2002), Constraints on future changes in climate and the hydrological cycle, *Nature*, *419*, 224–232.
- Boettger, T., et al. (2007), Wood cellulose preparation methods and mass spectrometric analyses of $\delta^{13}\text{C}$, $\delta^{18}\text{O}$ and non exchangeable $\delta^2\text{H}$ values in cellulose, sugar, and starch: An interlaboratory comparison, *Anal. Chem.*, *79*, 4603–4612.
- Büntgen, U., D. C. Frank, D. Nievergelt, and J. Esper (2006), Summer temperature variations in the European Alps, AD 755–2004, *J. Clim.*, *19/21*, 5606–5623.
- Casty, C., H. Wanner, J. Luterbacher, J. Esper, and R. Boehm (2005), Temperature and precipitation variability in the European Alps since 1500, *Int. J. Climatol.*, *25*, 1855–1880.
- Cook, E. R., and K. Peters (1981), The smoothing spline: A new approach to standardizing forest interior tree-ring width series for dendroclimatic studies, *Tree Ring Bull.*, *41*, 45–53.
- Dai, A., K. E. Trenberth, and T. Qian (2004), A global data set of Palmer Drought Severity Index for 1870–2002: Relationship with soil moisture and effects of surface warming, *J. Hydrometeorol.*, *5*, 1117–1130.
- Esper, J., E. R. Cook, and F. H. Schweingruber (2002), Low-frequency signals in long chronologies for reconstructing past temperature variability, *Science*, *295*, 2250–2253.
- Esper, J., R. J. S. Wilson, D. C. Frank, A. Moberg, H. Wanner, and J. Luterbacher (2005), Climate: Past ranges and future changes, *Quat. Sci. Rev.*, *24*, 2164–2166.
- Farquhar, G. D., M. H. O'Leary, and J. A. Berry (1982), On the relationship between carbon isotope discrimination and the intercellular carbon dioxide concentration in leaves, *Aust. J. Plant Physiol.*, *9*, 121–137.
- Frank, D., and J. Esper (2005), Temperature reconstructions and comparisons with instrumental data from a tree-ring network for the European Alps, *Int. J. Climatol.*, *25*, 1437–1454.
- Fritts, H. C. (1976), *Tree Rings and Climate*, 567 pp., Academic, New York.
- Gagen, M., D. McCarroll, and J.-L. Edouard (2004), Latewood width, maximum density, and stable carbon isotope ratios of pine as climate indicators in a dry subalpine environment, French Alps, *Arct. Antarct. Alp. Res.*, *36*, 166–171.
- Helle, G., and G. H. Schleser (2004), Beyond CO_2 -fixation by Rubisco: An interpretation of $^{13}\text{C}/^{12}\text{C}$ variations in tree rings from novel intra-seasonal studies on broad-leaf trees, *Plant Cell Environ.*, *27*, 367–380.
- Kagawa, A., A. Sugimoto, and T. C. Maximov (2006), Seasonal course of translocation, storage, and remobilization of ^{13}C pulse-labeled photoassimilate in naturally growing *Larix gmelinii* saplings, *New Phytol.*, *171*, 793–804.
- Leavitt, S. W., and A. Long (1984), Sampling strategy for stable carbon isotope analysis of tree rings in pine, *Nature*, *311*, 145–147.
- Loader, N. J., P. M. Santillo, J. P. Woodman-Ralph, J. E. Rolfe, M. A. Hall, M. Gagen, I. Robertson, R. Wilson, C. A. Froyd, and D. McCarroll (2007), Multiple stable isotopes from oak trees in southwestern Scotland and the potential for stable isotope dendroclimatology in maritime climatic regions, *Chem. Geol.*, in press.
- Luterbacher, J., D. Dietrich, E. Xoplaki, M. Grosjean, and H. Wanner (2004), European seasonal and annual temperature variability, trends, and extremes since 1500, *Science*, *303*, 1499–1503.
- Masson-Delmotte, V., et al. (2005), Changes in European precipitation seasonality and in drought frequencies revealed by a four-century-long tree-ring isotopic record from Brittany, France, *Clim. Dyn.*, *24*, 57–69.
- McCarroll, D., and N. J. Loader (2004), Stable isotopes in tree rings, *Quat. Sci. Rev.*, *23*, 771–801.
- Mitchell, T. D., and P. D. Jones (2005), An improved method of constructing a database of monthly climate observations and associated high-resolution grids, *Int. J. Clim.*, *693*–712.
- Pauling, A., J. Luterbacher, C. Casty, and H. Wanner (2006), Five hundred years of gridded high-resolution precipitation reconstructions over Europe and the connection to large-scale circulation, *Clim. Dyn.*, *26*, 387–405.
- Pederson, N., E. R. Cook, G. C. Jacoby, D. M. Peteet, and K. L. Griffin (2004), The influence of winter temperatures on the annual radial growth of six northern range margin tree species, *Dendrochronologia*, *22*, 7–29.

- Rafalli-Delerce, G., V. Masson, J. L. Dupouey, M. Stievenard, M. Breda, and M. Moisselin (2004), Reconstruction of summer droughts using tree-ring cellulose isotopes: A calibration study with living oaks from Brittany (western France), *Tellus, Ser. B*, *56*, 160–174.
- Richman, M. B. (1986), Rotation of principal components, *J. Clim.*, *6*, 293–335.
- Roden, J. S., G. Lin, and J. R. Ehleringer (2000), A mechanistic model for interpretation of hydrogen and oxygen isotope ratios in tree-ring cellulose, *Geochim. Cosmochim. Acta*, *64*, 21–35.
- Rozanski, K., L. Arguas-Arguas, and R. Gonfiantini (1993), Isotopic patterns in modern global precipitation, in *Climate Change in Continental Isotopic Records*, *Geophys. Monogr. Ser.*, vol. 78, edited by P. K. Swart et al., pp. 1–36, AGU, Washington, D. C.
- Saurer, M., K. Aellen, and R. Siegwolf (1997), Correlating $\delta^{13}\text{C}$ and $\delta^{18}\text{O}$ in cellulose of trees, *Plant Cell Environ.*, *20*, 1543–1550.
- Trenberth, K. E., and D. J. Shea (2005), Relationships between precipitation and surface temperature, *Geophys. Res. Lett.*, *32*, L14703, doi:10.1029/2005GL022760.
- Treydte, K., G. H. Schleser, F. H. Schweingruber, and M. Winiger (2001), The climatic significance of $\delta^{13}\text{C}$ in subalpine spruce (Lötschental, Swiss Alps): A case study with respect to altitude, exposure and soil moisture, *Tellus, Ser. B*, *53*, 593–611.
- Treydte, K., G. H. Schleser, G. Helle, D. Frank, M. Winiger, G. Haug, and J. Esper (2006), The 20th century was the wettest period in northern Pakistan over the past millennium, *Nature*, *440*, 1179–1182.
- van der Schrier, G., K. R. Briffa, P. D. Jones, and T. J. Osborn (2006), Summer moisture variability across Europe, *J. Clim.*, *19*, 2818–2834.
- Wells, N., S. Goddard, and M. J. Hayes (2004), A self-calibrating Palmer Drought Severity Index, *J. Clim.*, *17*, 2335–2351.
- Wilson, R. J. S., B. H. Luckman, and J. Esper (2005), A 500-year dendroclimatic reconstruction of spring/summer precipitation from the lower Bavarian forest region, Germany, *Int. J. Climatol.*, *25*, 611–630.
- Warren, C. R., J. F. McGrath, and M. A. Adams (2001), Water availability and carbon isotope discrimination in conifers, *Oecologia*, *127*, 476–486.
- Xoplaki, E., J. Luterbacher, H. Paeth, D. Dietrich, N. Steiner, M. Grosjean, and H. Wanner (2005), European spring and autumn temperature variability and change of extremes over the last half millennium, *Geophys. Res. Lett.*, *32*, L15713, doi:10.1029/2005GL023424.
- Yakir, D., and L. S. L. Sternberg (2000), The use of stable isotopes to study ecosystem gas exchange, *Oecologia*, *123*, 297–311.
- L. Andreu, E. Gutierrez, and O. Planells, Departamento d'Ecologia, Facultat de Biologia, Universitat de Barcelona, Av. Diagonal, 645, E-08028 Barcelona, Spain.
- Z. Bednarz, Department of Forest Botany, Agricultural University, 29 Listopada 46, PL-31425 Krakow, Poland.
- F. Berninger, Department of Biological Sciences, University of Quebec at Montreal, Montreal, QC, Canada H3C3P8.
- T. Boettger and M. Haupt, Department of Isotope Hydrology, UFZ-Helmholtz Centre for Environmental Research, Theodor-Lieser-Strasse 4, D-06120 Halle/Saale, Germany.
- J. Esper, D. Frank, and K. Treydte (corresponding author), Swiss Federal Research Institute WSL, Zürcherstr. 111, CH-8903 Birmensdorf, Switzerland. (kerstin.treydte@wsl.ch)
- N. Etien, M. T. Guillemin, V. Masson-Delmotte, M. Pierre, and M. Stievenard, Laboratoire des Sciences du Climat et de l'Environnement, L'Orme des Merisiers CEA Saclay IPSL/CEA/CNRS-UVSQ Bat 701, F-91191 Gif sur Yvette cedex, France.
- M. Filot and M. Leuenberger, Climate and Environmental Physics, Physics Institute, University of Bern, Sidlerstrasse 5, CH-3012 Bern, Switzerland.
- M. Grabner and M. Weigl, BOKU, University of Natural Resources and Applied Life Sciences, Peter Jordan-Strasse 82, A-1180 Wien, Austria.
- E. Hiltavuori, H. Jungner, and E. Sonninen, Dating Laboratory, University of Helsinki, POB64, FIN-00014 Helsinki, Finland.
- M. Kalela-Brundin, Museum of Forestry, Box 176, S-921 23 Lycksele, Sweden.
- M. Krapiec and E. Szychowska-Krapiec, Faculty of Geology, Geophysics and Environmental Protection, AGH University of Science and Technology, Mickiewicza 30, PL-30059 Krakow, Poland.
- N. J. Loader, Department of Geography, Swansea University, Singleton Park, Swansea SA2 8PP, UK.
- S. Pawelczyk, A. Pazdur, and M. Szczepanek, Institute of Physics, Silesian University of Technology, Krzywoustego 2, PL-44100 Gliwice, Poland.
- R. Pukiene, Kaunas Botanical Gardens Lab, Vytautas Magnus University, Kaunas 3018, Lithuania.
- C. E. Reynolds-Henne and M. Saurer, Paul Scherrer Institut, CH-5232 Villigen, Switzerland.
- K. T. Rinne, V. R. Switsur, and J. S. Waterhouse, Environmental Sciences Research Centre, Anglia Ruskin University, East Road, Cambridge CB1 1PT, UK.
- A. Saracino, Department of Arboriculture, Botany and Plant Pathology, University of Naples "Federico II", Via Università 100, I-80055 Portici, Italy.
- G. Helle and G. H. Schleser, Forschungszentrum Jülich GmbH, Leo-Brandt-Str., D-52425 Jülich, Germany.

C. M. D'Alessandro and L. Todaro, Department of Crop Systems, Forestry, and Environmental Sciences, Università della Basilicata, v.le Ateneo, Lucano, 10, I-85100 Potenza, Italy.

Supplementary Material

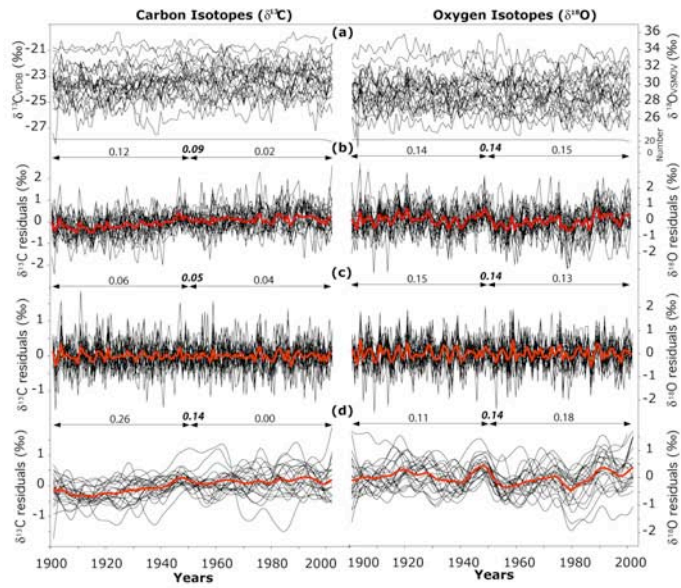
Signal strength and climate calibration of a European tree-ring isotope network

K. Treydte^{1*}, D. Frank¹, J. Esper¹, L. Andreu², Z. Bednarz³, F. Berninger⁴, T. Boettger⁵, C.D. D'Allessandro⁶, N. Etien⁷, M. Filot⁸, M. Grabner⁹, M. T. Guillemain⁷, E. Gutierrez², M. Haupt⁵, G. Helle¹⁰, E. Hilasvuori¹¹, H. Jungner¹¹, M. Kalela-Brundin¹¹, M. Krapiec¹², M. Leuenberger⁸, N.J. Loader¹³, V. Masson-Delmotte⁷, A. Pazdur¹⁴, S. Pawelczyk¹⁴, M. Pierre⁷, O. Planells², R. Pukiene¹⁵, C.E. Reynolds-Henne¹⁶, K.T. Rinne¹⁷, A. Saracino¹⁸, M. Saurer¹⁶, E. Sonninen¹¹, M. Stievenard⁷, V.R. Switsur¹⁷, M. Szczepanek¹⁴, E. Szychowska-Krapiec¹², L. Todaro⁶, J.S. Waterhouse¹⁷, M. Weigl⁹, G.H. Schleser¹⁰

Country	Site	Code	Coordinates Long/Lat	Altitude (m asl)	Species	$\delta^{13}\text{C}$ mean	$\delta^{18}\text{O}$ mean	TRW signal
Austria	Poellau	Poe	16.06, 47.95	500	<i>Pinus nigra</i>	-24.28	27.05	<i>Jul</i>
Austria	Lainzer Tiergarten	Lai	16.20, 48.18	300	<i>Quercus petraea</i>	-24.81	27.46	Jun
Finland	Bromarv	Bro	23.08, 60.00	5	<i>Quercus robur</i>	-24.83	25.62	JJ
Finland	Kessi, Inari	Ina	28.42, 68.93	150	<i>Pinus sylvestris</i>	-24.38	26.37	Jul
Finland	Sivakkovaara, Ilomantsi	Ilo	30.98, 62.98	200	<i>Pinus sylvestris</i>	-23.77	27.08	pJun
France	Rennes	Ren	-1.70, 48.25	100	<i>Quercus robur</i>	-24.82	30.21	Jul
France	Fontainebleau	Fon	2.67, 48.38	100	<i>Quercus petraea</i>	-23.81	30.47	<i>JA</i>
Germany	Dransfeld	Dra	9.78, 51.50	320	<i>Quercus petraea</i>	-23.50	28.68	AMJJAS
Italy	Serra di Crispo	Ser	16.20, 39.93	1900	<i>Pinus leucodermis</i>	-22.31	29.97	pMay
Lithuania	Panemunes Silas	Pan	23.97, 54.88	45	<i>Pinus sylvestris</i>	-22.96	28.67	Mar
Morocco	Col Du Zad	Col	-5.07, 32.97	2200	<i>Cedrus atlantica</i>	-20.61	32.72	<i>Oct</i>
Norway	Gutuli	Gut	12.18, 62.00	800	<i>Pinus sylvestris</i>	-23.36	27.62	Jul
Poland	Niepolomice, Gibiel	Nie2	20.38, 50.12	190	<i>Pinus sylvestris</i>	-25.71	27.74	Mar
Poland	Suwalki	Suw	22.93, 54.10	160	<i>Pinus sylvestris</i>	-23.18	28.42	MJJA
Poland	Niepolomice, Gibiel	Nie1	20.38, 50.12	190	<i>Quercus robur</i>	-22.73	29.26	pJun
Scotland	Lochwood	Lch	-3.43, 55.27	175	<i>Quercus robur</i>	-25.19	27.83	Jul
Spain	Massis del Pedraforca	Ped	1.70, 42.24	2120	<i>Pinus uncinata</i>	-21.98	30.80	pOct
Spain	Pinar de Lillo	Lil	-5.25, 43.07	1600	<i>Pinus sylvestris</i>	-22.29	30.81	pOct
Spain	Sierra de Cazorla	Caz	-2.96, 37.81	1820	<i>Pinus nigra</i>	-21.12	33.58	pJul
Switzerland	Cavergno	Cav	8.60, 46.35	900	<i>Quercus petraea</i>	-23.31	29.17	<i>Jun</i>
Switzerland	Vigera	Vig	8.77, 46.50	1400	<i>Pinus sylvestris</i>	-23.15	30.73	pMar
United Kingdom	Woburn	Wob	-0.59, 51.98	50	<i>Quercus robur</i>	-23.35	29.06	JJASO
United Kingdom	Windsor	Win	-0.59, 51.41	10	<i>Pinus sylvestris</i>	-22.92	30.33	pYear

Supplementary Table 1

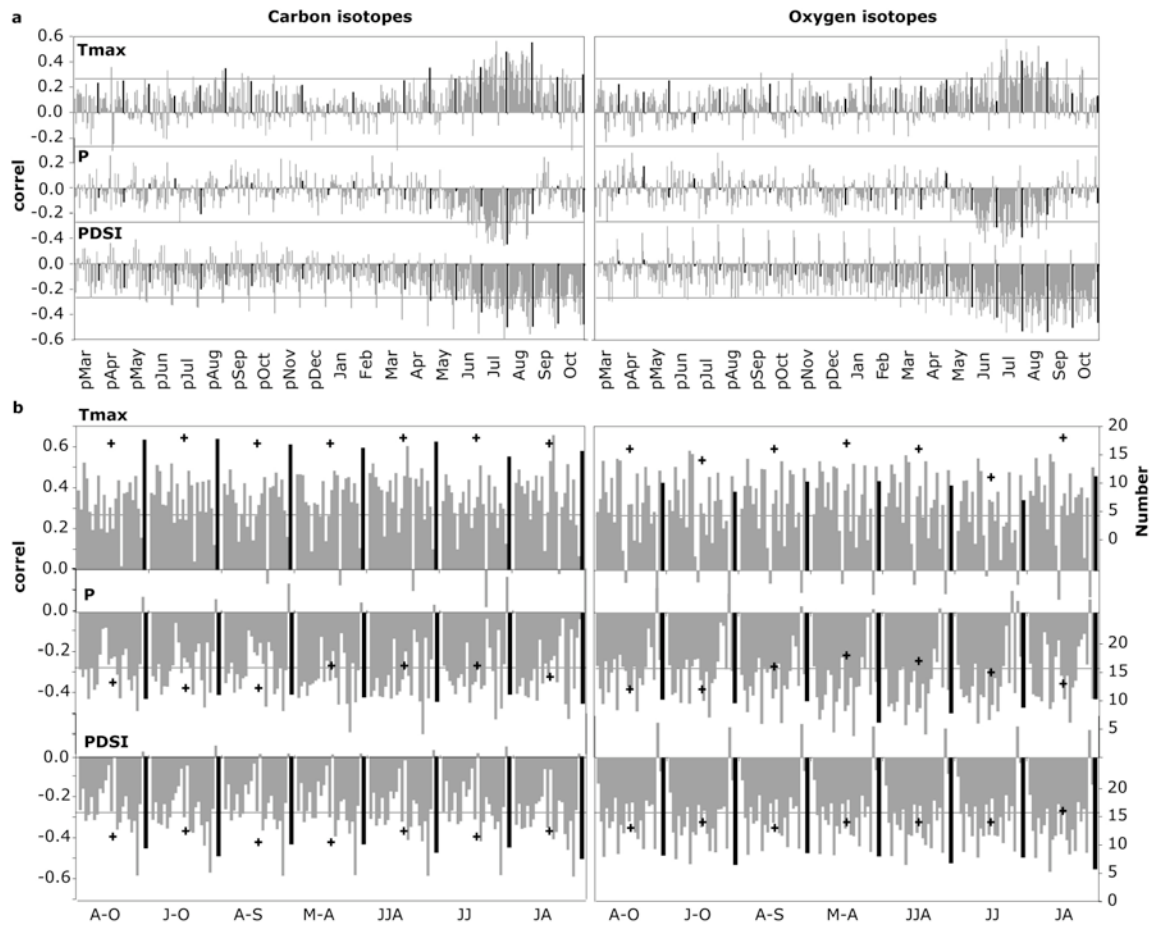
Site and species used in this study; $\delta^{13}\text{C}$ and $\delta^{18}\text{O}$ means are calculated over the common period AD 1901-1998, with bold being minimum values and bold italic being maximum values; "TRW signals" is the climate signal of tree-ring width for the month/season with highest correlation ($p < 0.05$): regular = precipitation, *italic* = *PDSI* and **bold** = **max. temperature**. Correlations were calculated after de-trending of individual ring-width series with 30-year splines.



Supplementary Figure 1

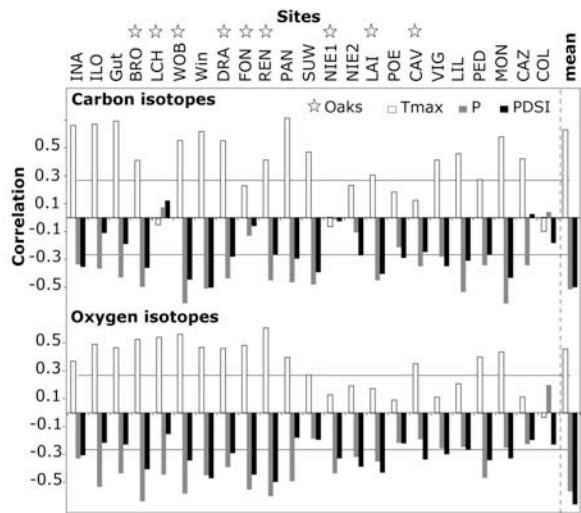
Carbon and oxygen isotope chronologies of all 23 sites considered in the network analysis; **a**: Raw data, with carbon isotopes corrected for changes in the atmospheric carbon isotope values; **b**: Standardized data as residuals from individual 20th century means (AD 1901-1998); **c**: High pass filtered data; **d**: Low pass filtered data (10-year splines); black solid lines in a indicate the replication over the 20th century; red are the averaged records over all sites; numbers are inter-site correlations (\bar{r}) based on averaging correlation coefficients between all records for the whole 1901-2002 period (***0.09***) and two independent time windows (AD 1901-1951 and AD 1952-2002).

Although \bar{r} s are generally low, they are - at least for the oxygen isotope network - in the range of \bar{r} s for summer precipitation data (June-August) at the same sites (0.12). With 0.34, \bar{r} s for summer maximum temperatures (June-August) are slightly higher.



Supplementary Figure 2

Monthly (**a**) and seasonal (**b**) correlations between isotope parameters and CRU meteo data; Tmax = maximum temperatures, P = precipitation, PDSI = Palmer drought severity index; grey bars represent correlations per site, black bars correlations between mean isotope records (averaged over all sites) and mean meteo data (averaged over corresponding grid cells); lines are $p < 0.01$ significance levels; crosses in the lower panel indicate the number of sites with significant correlations per season with A-O=April-October, J-O=June-October; A-S=April-September, M-A=May-August, JJA=June-August, JJ=June-July, JA=July-August; calculations are based on raw data and generally represent also high frequency correlations (see text)

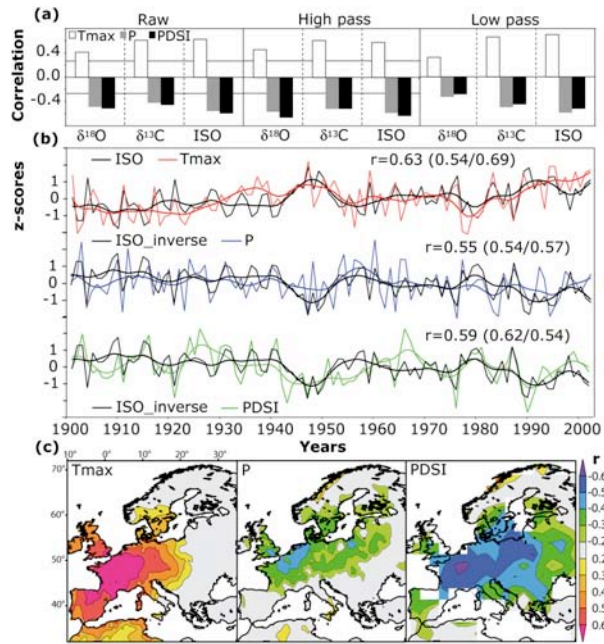


Supplementary Figure 3

June-August climate correlations of carbon and oxygen isotope chronologies on a site basis for high pass filtered data; for site information see supplement table 1; 'mean' are correlations between mean isotope records averaged over all sites and mean meteo data averaged over corresponding grid cells; lines are $p < 0.01$ significance levels

On combining the C and O networks

Being aware of the unsolved problem of unclear low frequency trends, we nevertheless used a rather coarse data treatment and averaged the mean and variance adjusted 'European' $\delta^{13}\text{C}$ and $\delta^{18}\text{O}$ records to a combined record 'ISO'. As shown in **Supplementary Figure 4**, using this new record surprisingly increases the climate correlations compared to the single isotope records. This is particularly the case for the raw, but also for the lp data, whereas in the hp data $\delta^{18}\text{O}$ -PDSI and $\delta^{13}\text{C}$ -Tmax relationships are slightly higher. We tested the temporal robustness of 'ISO' by splitting the record into two independent periods (1901-1951 and 1952-2002) (**SFig. 4b**). All correlations remain significant ($p < 0.01$), but r-values for temperature increase from the early to the recent period, values are constant for precipitation, and decrease for PDSI. The ISO-PDSI plot suggests that those differences mainly result from high frequency variations, since these are better captured in the early period. Nevertheless, longer-term trends are also preserved, particularly from the 1970s until present. This, however, is not pronounced in the correlation value. The warm period in the 1950s seems to capture temperature best, but currently cannot fully be explained through the climate variables and months used. Altogether, the correlation maps indicate that future climate reconstructions using a combined and optimized 'European' isotope record can be representative for a large area across Europe (**SFig. 4c**).



Supplementary Figure 4:

Climate response of the combined European isotope record 'ISO';
a: Correlation coefficients for raw, high pass and low pass filtered European $\delta^{18}\text{O}$, $\delta^{13}\text{C}$ and 'ISO' chronologies against June-August maximum temperatures (Tmax), precipitation (P) and PDSI; **b:** 'ISO' versus Tmax (red), P (blue) and PDSI (green) and correlation values for the full and early/recent calibration period (AD 1901-1951 and AD 1952-2002); thick lines represent 10-year splines; **c:** spatial correlation between 'ISO', Tmax, P and PDSI for June-August.